

LOCAL ENERGY MINIMISATIONS: AN OPTIMISATION FOR THE TOPOLOGICAL ACTIVE VOLUMES MODEL

N. Barreira, M.G. Penedo, M. Penas
VARPA Group, LFCIA, Dpto. Computación
Universidade da Coruña (Spain)

Keywords: Image segmentation, 3D reconstruction, active volumes, optimisation.

Abstract: The Topological Active Volumes (TAV) model (Barreira and Penedo, 2005) is a general active model focused on 3D segmentation tasks. It can also be used for the surface reconstruction and the topological analysis of the inner side of the detected objects. As any other deformable model, it defines a mesh and several energy functions. The minimisation of the energy functions moves the mesh towards the objects in the scene. The breaking of connections causes topological changes directed to the achievement of specific adjustments. This way, as well as improving the adjustment, the model is able to find several objects in the image and delimit holes in the structures detected. The TAV model achieves accurate results but the computational cost of the segmentation procedure is high. To reduce it, this paper proposes an optimisation of the model. It consists in performing local energy minimisations after the connection breaking process. This way, the execution times are reduced and the accuracy of the results is increased.

1 INTRODUCTION

Active models, also called deformable models, are widely used in image analysis to perform tasks such as image segmentation and shape recovery. They provide a general framework that can be applied to solve different problems in specific domains. Deformable models were introduced in 2D as explicit deformable contours (Kass et al., 1988) and they were generalised to the 3D domain (Terzopoulos et al., 1988). In the recent years, many deformable models have been developed to accomplish several tasks, mainly in medical images (Ferrant et al., 2001; Zhukov et al., 2002; Liu et al., 2003), or have been used in conjunction with other segmentation or optimisation methods (Magee et al., 2001; Fan et al., 2002). Nevertheless, all these models are mainly interested in surface extraction and shape recovery, not in the treatment of the whole detected solid.

The *Topological Active Volumes* model (Barreira and Penedo, 2005) is an active model focused on segmentation tasks that makes use of a volumetric distribution of nodes. It is fully automatic, so no *a priori* knowledge is needed to initialise the model. It also integrates information of edges and regions in the adjustment process and allows to obtain topological in-

formation inside the objects found. This way, the model, not only detects surfaces as any other active contour model, but also segments the inside of the objects. The model has a dynamic behaviour by means of topological changes in its structure, that enables accurate adjustments and the detection of several objects in the scene.

The main drawback of the Topological Active Volumes model is its high computational cost due to its structure and its generality. This paper proposes an optimisation of the model that increases its efficiency as well as improves the results of the segmentation process. This optimisation is based on the features of the model and the segmentation methodology. Furthermore, it can be used together with any other techniques to improve the efficiency of the segmentation procedure.

This paper is organised as follows. Section 2 describes the TAV model and the methodology used in the segmentation process. Section 3 explains the proposed optimisation method. Section 4 shows some results of the optimisation method. Finally, the conclusions are exposed in section 5.

2 TOPOLOGICAL ACTIVE VOLUMES

2.1 Model

The Topological Active Volumes (TAV) model (Barrera and Penedo, 2004) is an active contour model focused on extraction and modelisation of volumetric objects in a 3D scene.

A Topological Active Volume is a three-dimensional structure composed of interrelated nodes where the basic repeated structure is a cube. There are two kinds of nodes: the external nodes, that fit the surface of the object, and the internal nodes, that model its internal topology (figure 1). External nodes are related to edge information and internal nodes, to region information. The state of the model is governed by an energy function defined as follows:

$$E(v(r, s, t)) = \int_0^1 \int_0^1 \int_0^1 E_{int}(v(r, s, t)) + E_{ext}(v(r, s, t)) dr ds dt \quad (1)$$

where E_{int} and E_{ext} are the internal and the external energy of the TAV, respectively. The internal energy controls the shape and the structure of the net. Its calculation depends on first and second order derivatives that control contraction and bending, respectively. It is defined by the following equation:

$$E_{int}(v(r, s, t)) = \alpha(|v_r(r, s, t)|^2 + |v_s(r, s, t)|^2 + |v_t(r, s, t)|^2) + \beta(|v_{rr}(r, s, t)|^2 + |v_{ss}(r, s, t)|^2 + |v_{tt}(r, s, t)|^2) + 2\gamma(|v_{rs}(r, s, t)|^2 + |v_{rt}(r, s, t)|^2 + |v_{st}(r, s, t)|^2) \quad (2)$$

where subscripts represents partial derivatives and α , β and γ are coefficients controlling the first and second order smoothness of the net.

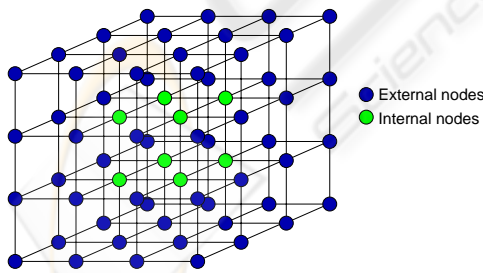


Figure 1: A TAV grid.

E_{ext} represents the features of the scene that guide the adjustment process and is different for external and internal nodes. It is defined as:

$$E_{ext}(v(r, s, t)) = \omega f[I(v(r, s, t))] + \frac{\rho}{|\mathcal{N}(r, s, t)|} \sum_{n \in \mathcal{N}(r, s, t)} \frac{1}{\|v(r, s, t) - v(n)\|} f[I(v(n))] \quad (3)$$

where ω and ρ are weights, $I(v(r, s, t))$ is the intensity value of the original image in the position $v(r, s, t)$, $\mathcal{N}(r, s, t)$ is the neighbourhood of the node (r, s, t) and f is a function of the image intensity, which is different for both types of nodes. For example, if the objects to detect are light and the background is dark, the energy of an internal node will be minimal when the node is on a point inside the object with a high grey level whereas the energy of an external node will be minimal when the node is on a discontinuity and on a dark point outside the object. In this situation, function f is defined as follows:

$$f[I(v(r, s, t))] = \begin{cases} \text{For internal nodes:} \\ h[I_{max} - \overline{I(v(r, s, t))}_N] \\ \text{For external nodes:} \\ h[\overline{I(v(r, s, t))}_N + \xi(G_{max} - G(v(r, s, t)))] \\ + DG(v(r, s, t)) \end{cases} \quad (4)$$

ξ is a weighting term, I_{max} and G_{max} are the maximum intensity values of image I and the gradient image G , respectively, $I(v(r, s, t))$ and $G(v(r, s, t))$ are the intensity values of the original image and gradient image in the position $v(r, s, t)$, $\overline{I(v(r, s, t))}_N$ is the mean intensity in a $N \times N \times N$ cube and h is an appropriate scaling function. $DG(v(r, s, t))$ is the distance from the position $v(r, s, t)$ to the nearest position in the gradient image that points out an edge.

2.2 Methodology

The TAV model is automatic, so the initialisation does not need any human interaction, opposed to other deformable models. The mesh is placed over the whole image and the nodes are located in such a way that the internodal distance is the same in each dimension. This way, the model can detect objects placed in different positions of the 3D image.

The adjustment process consists in the global energy minimisation of the mesh. A greedy algorithm is used for this task. The energy value for each TAV node is computed in several positions of the 3D image (the current position and its 26 neighbour positions) at every step of the minimisation process and the best one is chosen as the next position of the node. Once the mesh reaches a stable situation, this is, when the energy of each TAV node is minimal, the number of nodes is recomputed in order to adapt the TAV size to the object size. After that, the energy is minimised again.

To achieve a perfect adaptation, topological changes are performed in the mesh. These changes consist in connection breakings between external nodes badly placed, this is, external nodes that are not on the surfaces of the objects. The breaking of connections allows a perfect adjustment to the surfaces

and the detection of holes and several objects in the 3D scene. After each connection breaking, the TAV energy is globally minimised (Barreira and Penedo, 2005).

If there were several objects in the scene, a subTAV would be created for each one of them. A subTAV behaves like a TAV and repeats the process described above (Barreira and Penedo, 2004).

Figure 2 summarises the main stages of the TAV segmentation process.

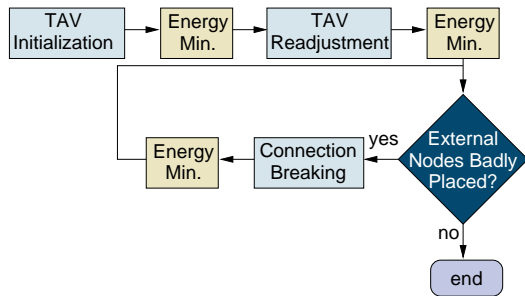


Figure 2: Main stages of the TAV segmentation process.

3 LOCAL ENERGY MINIMISATIONS

The global energy minimisation is an expensive task as it analyses every node in the mesh. On one hand, if the node is in a wrong position with a high energy value, it will be moved to another position with a lower energy value. On the other hand, if the node is correctly placed, it will stay in its current position. In both cases, a high number of computations will be performed but only the former computations are useful. So, performing only useful computations can improve the efficiency of the energy minimisation stages.

The minimisation stages after the initialisation and the readjustment phases (figure 2) cannot take advantage of this optimisation because most of the nodes are wrongly placed as the mesh was initiated in the previous stage and was not adjusted to the object. However, after each connection breaking stage there is another energy minimisation phase and, in this case, most of the TAV nodes are correctly placed since the energy of the mesh has been previously minimised. This way, the optimisation will be focused on the energy minimisation stages after the connection breakings. These minimisations are local because they are centred in the area where the connections are broken.

The key issue in the local energy minimisation procedure is the selection of the node set to minimise.

The energy equations and the relationships between nodes have been analysed in order to determine this set.

The energy of the node depends on the own node and its neighbours (equation 3). This implies that once the TAV energy is minimised, the node energies will not change unless some topological change that modifies the neighbourhood relationships among nodes is performed in the mesh. Then, if a connection is broken, the involved nodes will change its energy because they lose a neighbour, so their energies have to be minimised in order to find better positions for them. Moreover, if a node changes its position, the value of the function f can change because it depends on the position of the node (equation 4). If f modifies its value, not only the node will change its energy (equation 3), but also its neighbours will be affected since this f value is used to compute their energies (equation 3).

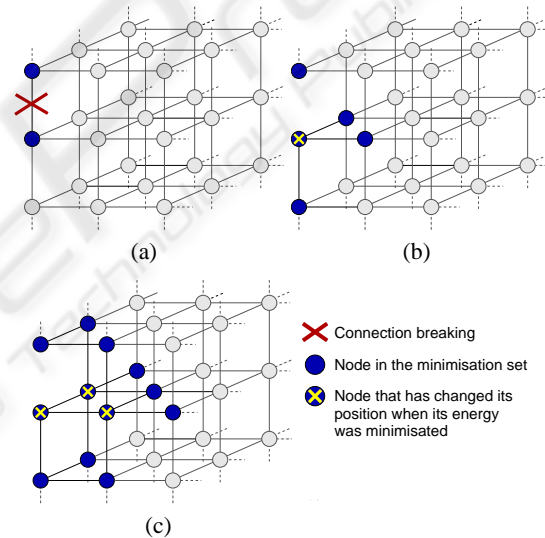


Figure 3: Nodes in the local minimisation set. (a) After the connection breaking. (b) After the first local energy minimisation step. The marked node has changed its position and its neighbours are added to the minimisation set. (c) After the second local energy minimisation step. The marked nodes have changed their positions so their neighbourhoods are included in the set.

As a result, the local energy minimisation procedure consists of the following steps:

1. Initialise a set with the nodes involved in the connection breaking
2. While the TAV energy is not minimal
 - (a) For each node in the set
 - i. Check several positions in order to minimise the node energy

- ii. Select the best position for the node
 - iii. If the node has changed its position, mark its neighbours
- (b) Add the marked neighbours to the set

Figure 3 shows an example of how the local energy minimisation method selects the nodes to perform the energy minimisation.

4 RESULTS

The local energy minimisation procedure was tested with several sets of 3D synthetic images and it was compared to the global energy minimisation method. To this end, each image was segmented by means of several TAV meshes using both methods. The same parameter set was used in each segmentation process and was empirically selected. This section presents some results obtained from both methods.

The first example is a 3D image with two objects. It was segmented using TAVs with 216, 400, 440, 528, and 624 nodes. The parameter set used was $\alpha = 2.5$, $\beta = 0.00001$, $\gamma = 0.00001$, $\omega = 3.0$, $\rho = 4.0$, and $\xi = 5.0$. The Sobel filter was applied to each 2D slice to obtain the gradient image. Figure 4 shows the results of the segmentation process and the execution times of the global and local energy minimisation methods. The local method's execution times are always smaller. However, with small meshes, it is common that a local minimisation affects to all the nodes so the time differences are not significant. But, as the number of nodes grows, the time differences are increased.

The second example is more complex than the first one. It was segmented with larger TAV meshes (729, 1728, 2744, 4096, and 5832 nodes). The parameter set used was $\alpha = 3.0$, $\beta = 0.00001$, $\gamma = 0.00001$, $\omega = 3.0$, $\rho = 3.0$, and $\xi = 5.0$. The gradient image was obtained with a 3D Canny filter (Canny, 1986). Figure 5 shows several views of the segmented figure and the execution times for the global and local energy minimisation methods. In this example, the execution times of the local method are lower, too.

Figure 6 shows the results of another segmentation example. The object was segmented using TAVs with 180, 847, 2304, and 4800 nodes. The values of the parameters were $\alpha = 3.5$, $\beta = 0.00001$, $\gamma = 0.00001$, $\omega = 4.0$, $\rho = 3.0$, and $\xi = 5.0$. The gradient image was obtained with a 3D Canny filter (Canny, 1986). In this example, the execution times of the local method are also lower than the execution times of the global method, as the chart in last row of figure 6 shows.

Figure 7 shows the results of another test set. The object was segmented using TAVs with 847, 1521, 2560, and 3564 nodes. The values of the parameters were $\alpha = 3.5$, $\beta = 0.00001$, $\gamma = 0.00001$, $\omega = 3.0$,

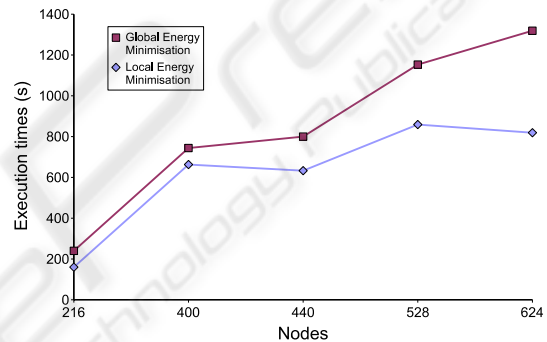
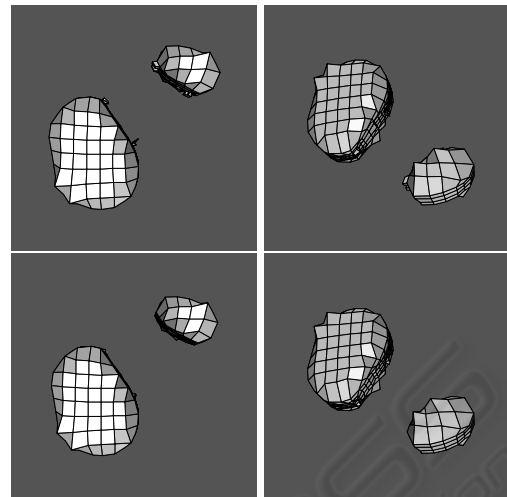


Figure 4: Results obtained on a simple example. The first and second rows show the surface reconstruction of the objects. They were segmented using a TAV with 824 nodes. The first row shows the results of the global energy minimisation and the second row, the results of the local energy minimisation. Last row shows the execution times of both methods using different TAV sizes.

$\rho = 3.0$, and $\xi = 5.0$. The gradient image was obtained with a 2D Sobel filter. Like the previous examples, the execution times of the local method are also lower than the results of the global method, as the chart in last row of figure 7 shows.

In each example, the results obtained by the alternative methods are very similar. Nevertheless, the local energy minimisation method obtains better results in most cases since the global minimisation method analyses the nodes in a sequential order whereas the local minimisation method follows a recursive order: first, the nodes involved in a connection breaking minimise their energies, then their neighbours, then the neighbours of these neighbours, and so on. This fact allows the mesh to achieve a natural adaptation to the surfaces which improves the adjustment. The final energy of the mesh can be used to measure the adjust-

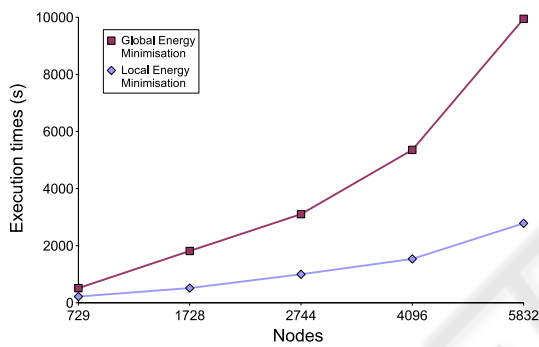
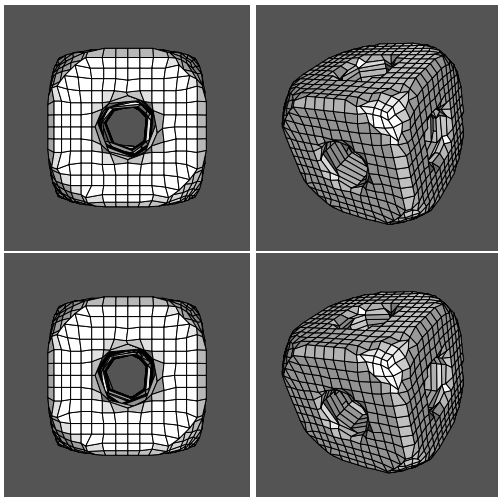


Figure 5: Results obtained on a complex example. The first and second rows show the surface reconstruction of the object using the global minimisation and the local minimisation, respectively. The object was segmented using a TAV with 4096 nodes. Last row shows the execution times of both methods using different TAV sizes.

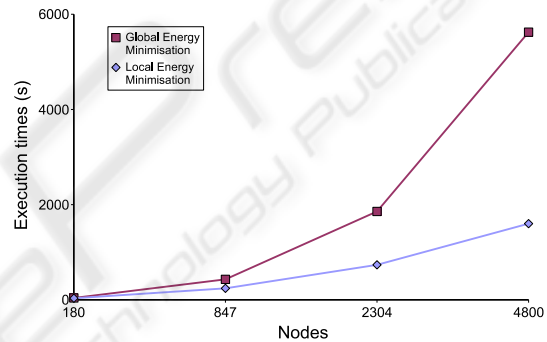
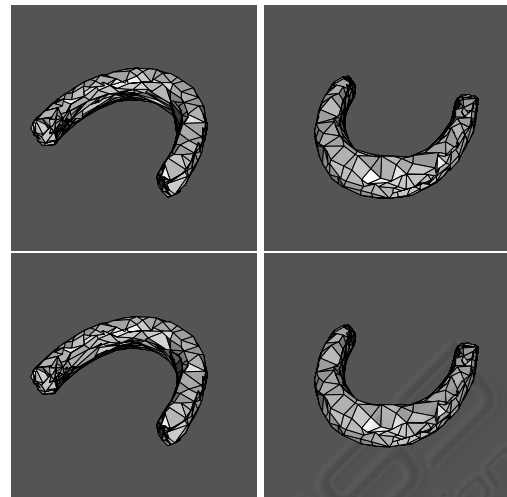


Figure 6: Results obtained on another test set. The surface reconstruction of the object is shown in the first and second rows. The object was segmented using a TAV with 4096 nodes. The first row shows the results of the global energy minimisation and the second row, the results of the local energy minimisation. Last row shows the execution times of both methods using different TAV sizes.

ment of the TAV to the target object since the adjustment process is an energy minimisation process. This means that a lower energy value indicates a better adjustment. Table 1 shows the normalised final energies of the meshes used for the test sets. Most of the values obtained with the local energy minimisation method are lower than the values obtained with the global method, so the adjustment with the local method is generally more accurate than the adjustment with the global method.

5 CONCLUSIONS

This paper presents an optimisation of the TAV model. It consists in performing local energy minimisations after each connection breaking stage instead

of global energy minimisations. This way, the number of useless computations is reduced and the efficiency of the segmentation process is increased. Nevertheless, the efficiency of the proposed method lies mainly on the complexity of the segmented objects. Thus, if most of the mesh nodes are wrongly placed due to object features, the local minimisation process can involve the whole mesh and the behaviour of the local approach can be equal to the global one.

The local energy minimisation method was used together with a greedy algorithm but it can be used with any other minimisation algorithm as it only limits the set of nodes to minimise and has no influence on the minimisation algorithm. For the same reason, the TAV parameter set is not affected by the local minimisation process.

The local minimisation method was tested with se-

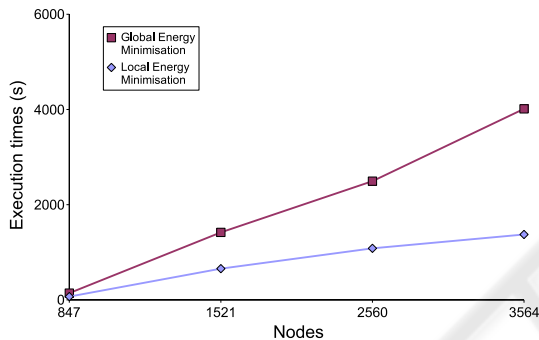
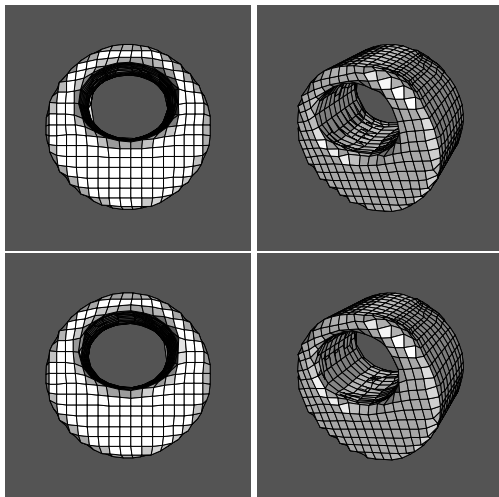


Figure 7: Results obtained on another example. The first and second rows show the surface reconstruction of the object. It was segmented using a TAV with 3564 nodes. The first row shows the results of the global energy minimisation and the second one, the results of the local energy minimisation. Last row shows the execution times of both methods using different TAV sizes.

veral sets of 3D images. The execution times were clearly reduced and the results obtained were slightly improved. The time differences grow exponentially with the number of nodes since the breakings tend to affect a lower percentage of nodes as the number of nodes is increased.

Future work in the TAV optimisation field includes the definition of more efficient minimisation algorithms, the use of information from the domain to guide the adjustment process when the model is applied to a specific field, and the parallelisation of the energy minimisation stage.

REFERENCES

Barreira, N. and Penedo, M. G. (2004). Topological Active Volumes for Segmentation and Shape Reconstruction

of Medical Images. *Image Analysis and Recognition: Lecture Notes in Computer Science*, 3212:43–50.

Barreira, N. and Penedo, M. G. (2005). Topological Active Volumes. *EURASIP Journal on Applied Signal Processing*, 13(1):1937–1947.

Canny, J. (1986). A computational approach to edge-detection. *IEEE Trans. on Pattern Analysis and Machine Intelligence*, 8(6):679–698.

Fan, Y., Jiang, T., and Evans, D. J. (2002). Volumetric Segmentation of Brain Images Using Parallel Genetic Algorithms. *IEEE Transactions on Medical Imaging*, 21(8):904–909.

Ferrant, M., Cuisenaire, O., Macq, B., Thiran, J., Shenton, M., Kikinis, R., and Warfield, S. (2001). Surface based atlas matching of the brain using deformable surfaces and volumetric finite elements. In *MICCAI 2001*, pages pp. 1352–1353.

Kass, M., Witkin, A., and Terzopoulos, D. (1988). Active contour models. *International Journal of Computer Vision*, 1(2):321–323.

Liu, R., Shang, Y., Sachse, F. B., and Dssel, O. (2003). 3D active surface method for segmentation of medical image data: Assessment of different image forces. In *Biomedizinische Technik*, volume 48-1, pages 28–29.

Magee, D. R., Bulpitt, A. J., and Berry, E. (2001). Combining 3d deformable models and level set methods for the segmentation of abdominal aortic aneurysms. In *BMVC*.

Terzopoulos, D., Witkin, A., and Kass, M. (1988). Constraints on deformable models: Recovering 3D shape and nonrigid motion. *Artificial Intelligence*, 36(1):91–123.

Zhukov, L., J. Bao, I. G., Wood, J., and Breen, D. (2002). Dynamic deformable models for mri heart segmentation. In *SPIE Medical Imaging 2002*.

Table 1: Normalised TAV energies obtained in the segmentation processes of the examples.

		TAV nodes - first example				
		216	400	440	528	624
Global min.		0,583	0,757	0,787	0,885	1
Local min.		0,540	0,745	0,780	0,881	0,952
		TAV nodes - second example				
		729	1728	2744	4096	5832
Global min.		0,366	0,512	0,663	0,817	0,992
Local min.		0,365	0,511	0,665	0,816	1
		TAV nodes - third example				
		180	847	2304	4800	
Global min.		0,130	0,336	0,600	1	
Local min.		0,140	0,344	0,581	0,959	
		TAV nodes - fourth example				
		847	1521	2560	3564	
Global min.		0,511	0,622	0,832	1	
Local min.		0,511	0,621	0,837	0,995	